Delivery of nematicides using TMGMV-derived spherical nanoparticles

Adam A. Caparco[a], Ivonne Gonzalez-Gamboa[a], Samuel S. Hays[a], Jonathan K. Pokorski[a,e], Nicole F. Steinmetz[a-g]*

[a]Department of NanoEngineering, University of California, San Diego, La Jolla, CA, USA 92093

[b]Department of Bioengineering, University of California, San Diego, La Jolla, CA, USA 92093

[c]Department of Radiology, University of California, San Diego, La Jolla, CA, USA 92093

[d]Center for Nano-ImmunoEngineering, University of California, San Diego, La Jolla, CA, USA 92093

[e]Institute for Materials Discovery and Design, University of California, San Diego, La Jolla, CA, USA 92093

[f]Moores Cancer Center, University of California, San Diego, La Jolla, CA, USA 92093

[g]Center for Engineering in Cancer, Institute for Engineering in Medicine, University of California, San Diego, La Jolla, CA, USA 92093

*corresponding author: nsteinmetz@ucsd.edu

ABSTRACT

Spherical nanoparticles (SNPs) from tobacco mild green mosaic virus (TMGMV) were developed, characterized, and their application for agrochemical delivery was demonstrated. Specifically, we set out to develop a platform for pesticide delivery targeting nematode in the rhizosphere. SNPs were obtained by thermal shape-switching of the TMGMV. We demonstrated that cargo can be loaded into the SNPs during

thermal shape-switching, enabling one-pot synthesis of functionalized nanocarriers. Cyanine 5 and ivermectin were encapsulated into SNPs achieving 10% mass loading. SNPs demonstrated good mobility and slightly higher soil retention than TMGMV rods. Ivermectin delivery to *Caenorhabditis elegans* using SNPs was determined after passing the formulations through soil. Using a gel burrowing assay, we demonstrate potent efficacy of SNP-delivered ivermectin against nematodes. Like many pesticides, free ivermectin is adsorbed in the soil and did not show efficacy. The SNP nanotechnology offers good soil mobility and a platform technology for pesticide delivery to the rhizosphere.

Keywords: precision farming, agricultural nanotechnology, nematicide delivery, ivermectin, tobacco mild green mosaic virus, spherical nanoparticles

MAIN TEXT

As the global population increases, strategies to protect crops are essential for meeting the forthcoming demand for food. A particular challenge are plant parasitic nematodes accounting for $125B USD financial losses and 14% of crops losses each year worldwide[1]. Pesticide use has overcome some challenges, but introduces new challenges in human health, environmental toxicity, and skepticism among the public. Compounded with a robust regulatory environment, creating next-generation (nano)pesticides is an essential step in creating a sustainable agricultural system.

Contemporary nematode management makes use of non-fumigant nematicides, but their effectiveness is limited by their slow diffusion through soil, which leads to higher doses being used and thus chemical contamination of the crops, soil, and groundwater – ultimately putting our health at risk[2]. Following the concepts of nanomedicine, the encapsulation of nematicides in nanoparticles has been proposed to reduce exposure risks while enhancing the efficacy of nematicides at the root level[3]. Nanoparticle technology

offers pathogen-targeted delivery, while protecting the active ingredient from premature biodegradation and photolysis[4]. Synthetic nanoparticles have been proposed[5]; however, manufacturing costs, biodegradability and safety issues must be addressed when introducing synthetic materials into the environment[6].

We propose plant virus-based pesticide nanocarriers as an alternative to synthetic nanoparticles. Plant viruses evolved to be stable in soil, some are soil-born and many are transmitted by nematode vectors[7, 8]. We seek to repurpose plant virus as carriers for pesticides targeting plant parasitic nematodes. In previous work, we and others demonstrated these concepts: red clover necrotic mottle virus (RCNMV) has been developed for nematicide delivery and effective treatment of tomato seedlings infested with the root-knot nematode *Meloidogyne hapla* was demonstrated using RCNMV particles carrying avermectin[9]. And we began development of tobacco mild green mosaic virus (TMGMV) as a pesticide carrier demonstrating facile chemistry to enable active ingredient loading covalent attachment[10]. TMGMV has good soil mobility outperforming other plant viruses or synthetic nanoparticles[11]. Our motivation and rationale to use TMGMV as a platform technology is as follows: TMGMV is already approved by the EPA, and Solvinix™ (a formulation of TMGMV mass-produced by BioProdex) is used as a bioherbicide for the control of the invasive weed tropical soda apple [12-14]. TMGMV is not transmitted by insects, pollen, or other vectors; it is not seed borne and cannot self-disseminate. Furthermore, plant viruses offer unparalleled engineering design space; for example, using tobacco mosaic virus, it was demonstrated that bottom-up assembly using the coat protein (CP) and designer RNA templates yielded longer and shorter nanotubes, spheres, and complex shapes such as stars and boomerangs[15].

Building on this prior work, we set out to develop a platform technology for pesticide delivery to the rhizosphere. While successful, covalent conjugation of agrochemicals to TMGMV proved challenging even with extensive formulation chemistry[16]. From discussions with industry, it is noted that chemical conjugation of the active ingredient is not desired, because modifications to the agrochemical initiate new

regulatory approval and registration processes. Therefore, we thought to explore whether the active ingredient could be loaded efficiently during a thermal shape-switching process of TMGMV. We draw from reports that highlight that Tobacco mosaic virus (TMV), *Alternathera* mosaic virus (AltMV), and Potato virus X (PVX) – all of which form high aspect ratio nanotubes, could be transitioned into spherical nanoparticles (SNPs) upon exposure to heat[17-19]. The transformation occurs while heating well above the melting temperature of the nucleoprotein assembly, causing unfolding and potentially reassembly into ordered aggregates which assume spherical shape. We hypothesized that agrochemical cargo could be encapsulated into SNPs formed from TMGMV during this shape transition. The advantage of the SNP technology is that SNPs are devoid of RNA and therefore non-infectious toward crops[19]. Here, we developed the protocols for SNP formulation from TMGMV. We characterized the structural properties of the SNPs and assessed their loading capacity by making use of a fluorophore (Cyanine 5) and a nematicide (ivermectin). We demonstrated soil mobility and efficacy against *Caenorhabditis elegans*, a model organism for plant-parasitic nematodes, by treatment with ivermectin in SNPs.

SNPs can be generated from high aspect ratio plant viruses, but optimization is needed for each system[19-22]. We investigated a phase space for TMGMV rod-to-SNP transition (**Figure 1**). We varied TMGMV concentration, heating time, and temperature and confirmed the nanoparticle morphology by SEM (**Figure 1a-e** shows data for TMGMV at 5 mg mL^{-1}, remaining conditions are shown in **Figure S1a,b)**. SNPs formed at all tested TMGMV concentrations but required a minimum temperature and heating time to completely transition. Below 80 °C, SNPs did not form within 1 minute of heating, instead forming agglomerated rod bundles (**Figure S1c**). Above 90 °C, SNPs formed after 30 seconds of heating. For temperatures and heating times below this threshold, aligned and agglomerated TMGMV bundles were observed (**Figures 1c** and **S1c**). At the threshold of 30 seconds at 96 °C, SNPs were formed, and the SNP diameter was proportional to the initial TMGMV concentration; at 0.1 mg mL^{-1} of TMGMV, SNPs were 100-200 nm in diameter; the largest SNPs – up to 2 μm in diameter – were obtained when concentrations were increased up to 10 mg mL^{-1} (**Figure 1e** and **Figure S2**).

Based on prior studies by Atabekov *et al.*, it is hypothesized that SNPs form by partial or full dissociation of the nucleoprotein rods at high temperatures with the SNP size being proportional to the starting protein concentration. For TMV, the rods swell at their head and tail into spherical units; at the same time TMV rods bundle and cluster upon heating, suggesting both intra- and interparticle forces drive assembly[19]. In agreement with the prior observations, we found our TMGMV SNPs could be produced in a range of sizes and colloidal suspensions by varying the starting concentration of the TMGMV rods. We also observed transition incomplete spheres and irregularly shaped clusters, when the heating conditions were not sufficiently high or long (**Figure S1**), suggesting the total thermal energy transferred is important for complete shape transition.

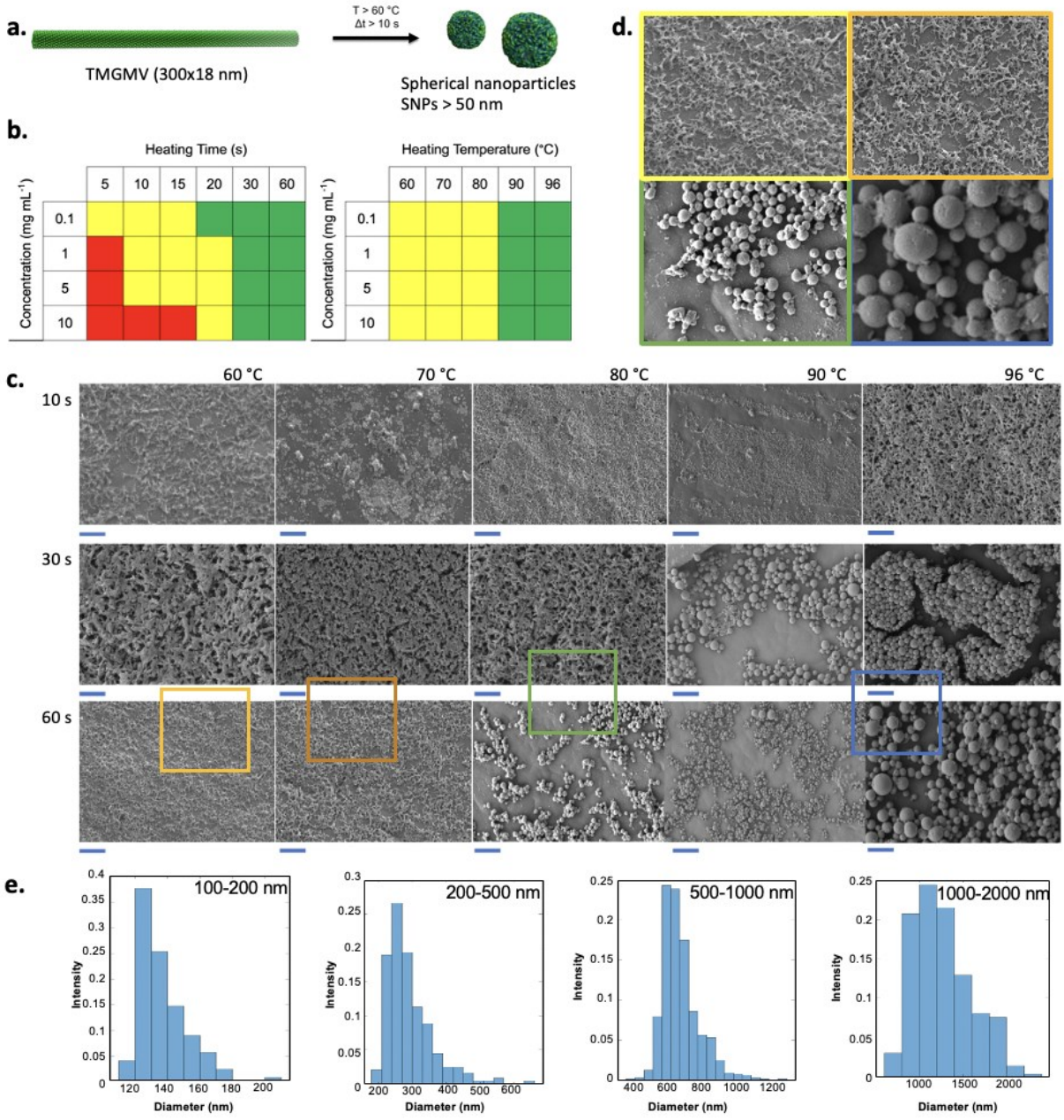

Figure 1. A schematic representation of thermally induced rod-to-SNP transition of TMGMV (a). A representative phase space of TMGMV-to-SNP transition at 96 °C (b, left) and at 30 s of heating time (b, right), with red indicating no formation, yellow indicating partial transformation, and green indicating reliable SNP formation. A phase space of TMGMV/SNP morphology at 5 mg mL^{-1} initial TMGMV concentration after heating for 10-60 s and temperature ranges from 60-96 °C; scale bars represent 2 µm (c). A zoomed in view to demonstrate nanoparticle features of the colored boxes in the phase space (d). Size distributions for four different preparations of TMGMV SNPs (e); see also **Figure S2**.

We characterized the SNP protein content by SDS-PAGE and LC-MS-MS. SDS-PAGE indicated differentiation between TMGMV rods and their SNPs (**Figure S3**): TMGMV consists of ~ 2100 copies of an identical coat protein (CP) with a molecular weight of 17.6 kDa. SNPs samples show the CP, and in addition a dimeric CP (35 kDa) and a smaller degradation byproduct (15 kDa). In the absence of protease or bacterial contamination, the cleaved protein sequence was unexpected. LC-MS-MS and sequence analysis identified this band as derived from the TMGMV CP. Interestingly this phenomenon has not been described for any rod-to-SNP transition[17-19]. Aspartic acid-proline (DP) bonds in proteins can be susceptible to cleavage at temperatures close to 100°C and in acidic conditions[23-25]. Therefore, we analyzed the sequences of TMGMV and other rod-shaped viruses with reported SNP transition. TMV and TMGMV both have a DP at amino acid position D20-P21, while PVX and AltMV do not have this motif. The length of the N-terminal sequence before the putative cleavage site is 2.1 kDa, correlating with the mass shift in SDS-PAGE. This cleavage effect is reported to occur at longer heating times, on the order of minutes. Because the transition of TMGMV to SNPs takes longer than TMV, it is possible this phenomenon can occur with TMV and has not yet been observed.

Soil delivery of hydrophobic small molecule pesticides suffers from poor soil mobility and rapid washout effects, necessitating a delivery vehicle to remain effective and economically viable[26-29]. In prior work, we demonstrated that TMGMV has good soil mobility properties – outperforming other synthetic and biological systems and we attributed this to the zwitterionic nature of the protein-based macromolecules [28]. We mirrored the prior experimental set up for our soil mobility assays with SNPs[28]. In brief, a 0.3 cm diameter column was packed with Magic topsoil gardening soil (Michigan Peat) to a depth of 10 cm and pre-wetted before a bolus application of TMGMV or SNPs (0.5 mg in 1 mL DI H_2O, irrigated at 5 mL min^{-1}). Fractions were collected and analyzed by SDS-PAGE to determine their elution profile (**Figure 2** and **Figure S4**). SNPs have good soil mobility independent of their size (**Figure 2c**), and the SNPs display a longer elution volume (8-10 mL) compared to TMGMV (~6 mL). This is likely due to their larger length scale and change in surface chemistry of SNPs compared to rods facilitating

more interactions between the particles and the soil[30]. Convection of the fluid traveling may affect the mobility of nanoparticles, essentially dragging the nanoparticles with it through porous channels in the soil – which may explain the size-independent soil mobility of the SNPs (100 nm-2 μm). This is corroborated by the dispersion and peak broadening seen for smaller particles where diffusion may begin to determine the flow behavior more. Likely a combination of both convection and diffusion determines the mobility behavior of nanoparticles in soil and will require more detailed investigation.

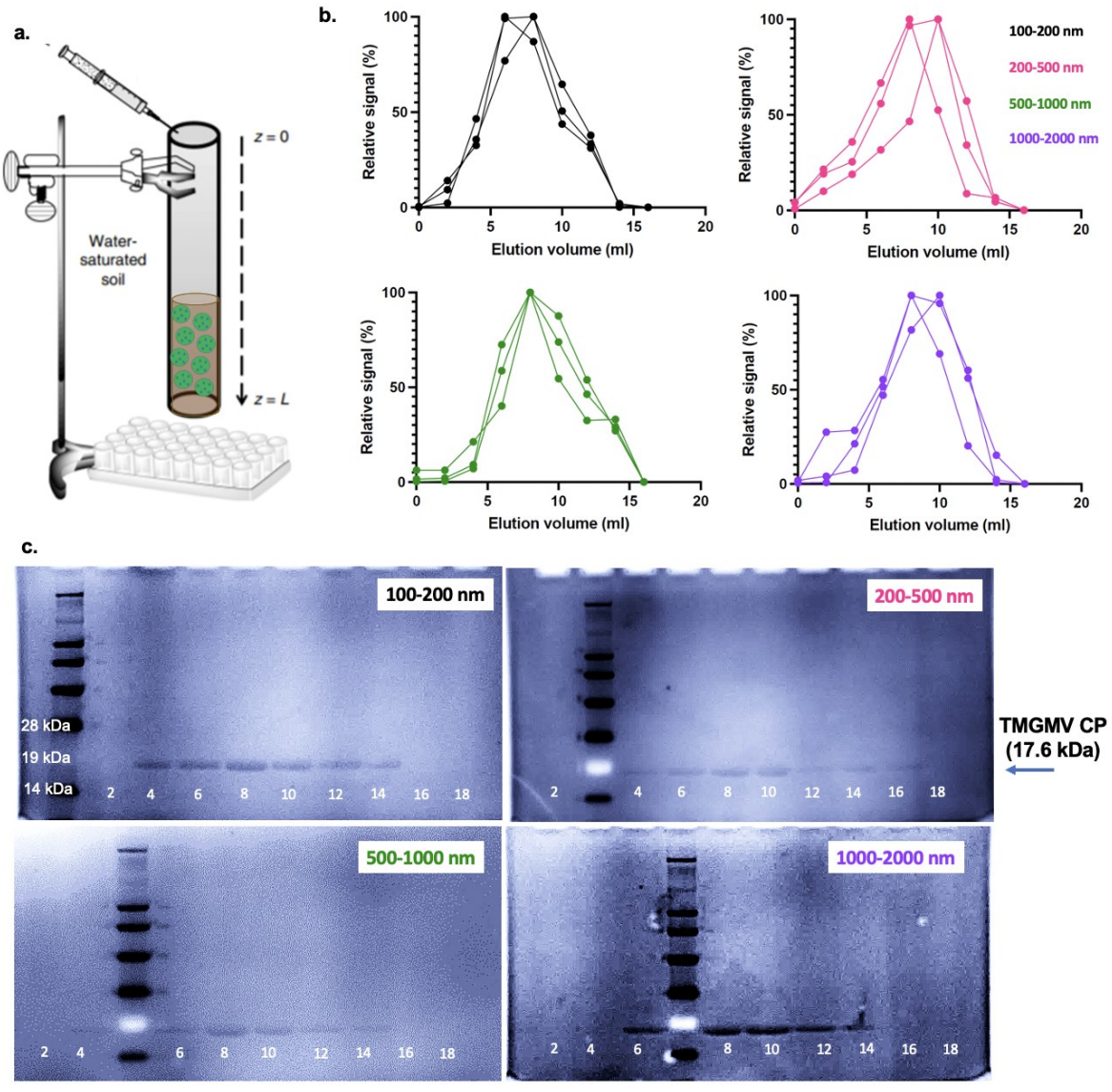

Figure 2. **SNPs demonstrate good soil mobility.** (a) A schematic of SNP soil mobility measurements in 10 cm soil columns (not to scale). (b) Fractions (2 mL) were collected and analyzed by SDS-PAGE (c); band intensity was calculated and is plotted. Four distinct SNP formulations were analyzed SNP measuring 100-200 nm ($SNP_{100\text{-}200}$), 200-500 nm ($SNP_{200\text{-}500}$), 500-1000 nm ($SNP_{500\text{-}1000}$), and 1000-2000 nm ($SNP_{1000\text{-}2000}$); three independent trials are plotted for each condition. There were no statistically significant differences comparing the different sized SNP batches (ANOVA).

For active ingredient encapsulation studies, we selected the 60 sec/96 °C condition and varied TMGMV starting concentration (0.1, 1.0, 5.0, and 10 mg mL^{-1}). Ivermectin was used as the nematicide and Cyanine 5 (Cy5) served as a photostable and heat stable fluorophore[31]. Small molecule loading into SNPs derived from TMV and other viruses has been demonstrated[17, 18, 20, 22]. However, these systems relied on chemical conjugation strategies. In the agricultural setting this is undesired, because changing the chemical structure of the active ingredient requires new active ingredient registration. Also, bioconjugation procedures are often multi-step processes requiring repeated purification steps, therefore reducing yields, while increasing costs. A one-step synthesis of active-laden SNPs may mitigate these technological hurdles (outlined in **Figure 3a**).

a.

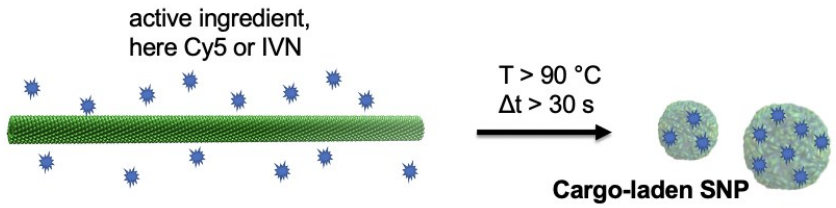

b.

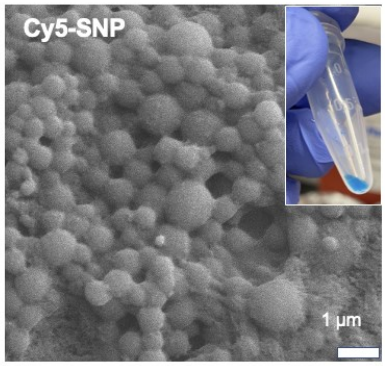

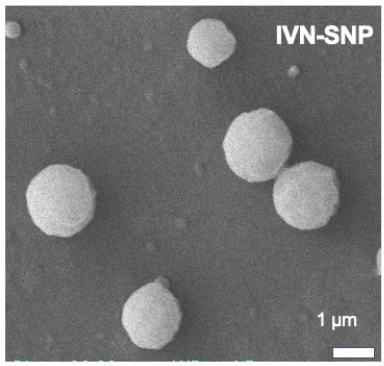

c.

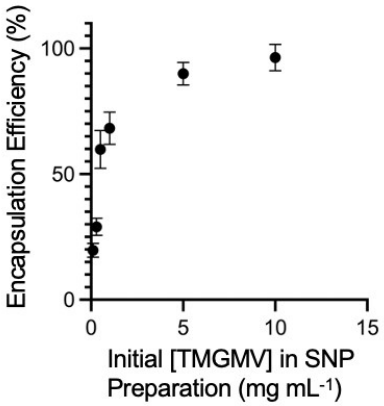

d.

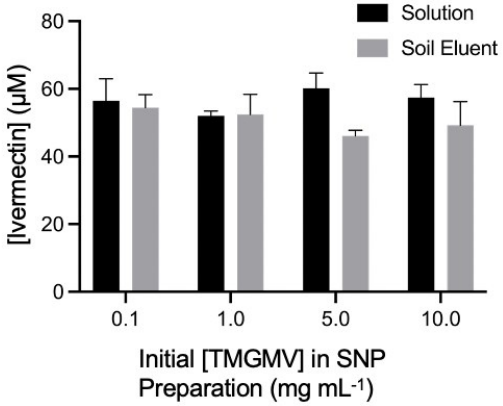

e.

TMGMV (mg mL^{-1})	SNP Diameter (nm)	Cy5 per CP	Ivermectin per CP
0.1	100-200	77 ± 11	48 ± 5
1	200-500	27 ± 4	17 ± 3
5	500-1000	7 ± 1	5 ± 1
10	1000-2000	4 ± 0.3	3 ± 0.2

f.

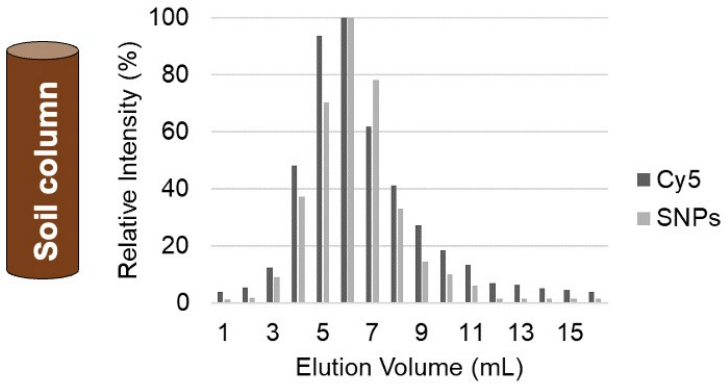

Figure 3. Encapsulation of small molecules (active ingredient, Cy5 or ivermectin, IVN) during the thermal shape-switching of TMGMV to SNPs (transparency to indicate small molecules are inside SNPs) (a). SEM micrographs of Cy5-SNPs (with blue pellet of Cy5-SNPs, inset) and IVN-SNP (b). The encapsulation efficiency of Cy5 (1 mg mL^{-1}) in TMGMV SNPs at several concentrations of TMGMV (c). Competitive ELISA results for ivermectin loading in SNPs (samples prepared to be 50 μM, N = 3) (d). Quantitative data of Cy5 and ivermectin per TMGMV (N = 3) (e). Overlapping soil mobility of Cy5 signal and SNP signal as a function of elution volume in a 10 cm soil column (f).

A fixed concentration of Cy5 (1 mg mL^{-1}) was added during the thermal transition (60 s, 96 °C) of TMGMV to SNP (achieving a Cy5 to protein mass ratio of 0.1- to 10). Cy5-SNPs were purified using spin filters to remove excess Cy5. The purified Cy5-SNPs were visibly concentrated with Cy5 (**Figure 3b**, inset). SEM imaging indicated no apparent differences in the morphology of Cy5-SNPs compared to the non-loaded SNPs (**Figure 3b**). Fewer non-SNP aggregates were observed, which may be attributed to the 5% by volume of DMSO added during synthesis, which may aid in the dissociation and thermal transformation of SNPs. Absorbance readings (at 647 nm) indicated concentration-dependent removal of Cy5 (1 mg mL^{-1}) from the solution into the SNP phase, with removal efficiencies ranging from 25% for 0.1 mg mL^{-1} TMGMV to nearly 100% for 10 mg mL^{-1} TMGMV (**Figure 3c,e**). We demonstrate cargo-laden SNPs of distinct sizes from 100-200 nm to 500 nm-2 μm can be obtained in a one-step synthesis that does not require chemical alteration of the cargo. For Cy5, 77 molecules per CP were loaded in the 100-200 nm Cy5-SNPs (0.1 mg mL^{-1} TMGMV). As TMGMV concentration and particle size increased, the amount of Cy5 per CP trended downward to fewer than 10 molecules per CP for the largest particles (500 nm-2 μm), still exceeding the maximum achieved through bioconjugation without and optimization.

Next, ivermectin was encapsulated. When we heated aqueous TMGMV solutions containing ivermectin, we observed the formation of a fluffy colloidal byproduct which interfered with SNP formation (**Figure S5**). This byproduct formed regardless of the presence or absence of TMGMV, identifying it as an aggregate of ivermectin. To increase the solubility of ivermectin and enable SNP

entrapment, we added 25% by volume acetonitrile as a cosolvent. This strategy was successful resulting in ivermectin-laden SNPs (**Figure 3b** and **S5**). The cosolvent and excess ivermectin was then removed using spin filtration. To quantify ivermectin, a competitive ELISA was used (**Figure 3d,e** and **Figure S6**). Up to ~50 ivermectin molecules per CP were quantified for SNPs measuring 100-200 nm (0.1 mg mL^{-1} TMGMV). For the smaller SNPs (100-200 nm), the estimated loading per SNP is on the order of $1x10^6$ ivermectin per SNP, or 60% ivermectin by mass.

To gain insights into the structural changes that occur during SNP formation with cosolvent, circular dichroism (CD) spectra comparing IVN-SNP vs. TMGMV were analyzed (**Figure S7**). When comparing TMGMV rods to SNPs, a change in intensity of signal around 200-220 nm and a peak maximum shift from 270 nm to 260 nm after the thermal transition was apparent. Shifts associated with SNP formation are exacerbated in the presence of acetonitrile as a cosolvent, but acetonitrile without heating shows little effect on CD spectra. Additionally, the presence of ivermectin leaves a spectral fingerprint at 240-260 nm. Thus data indicates changes in secondary structure during SNP formation.

Next, we confirmed soil mobility of the cargo-laden SNPs and the elution maxima matched with the empty SNPs, indicating that the cargo does not impact soil mobility (**Figure 3f** and **Figure S8**). More importantly, we confirmed in 10 cm soil columns, Cy5 (cargo) and SNP (carrier) coeluted from the soil columns and this held true for all sizes tested. This indicates that the non-covalent loading of cargo into SNPs allows transport through soil. This is in stark contrast for the TMGMV rods: we previously established non-covalent loading strategies by making use of electrostatic binding, while stable in the test tube, we found the cargo to be stripped of the particle in soil[32].

As a final test, we evaluated the efficacy of IVN-SNPs vs. free IVN against *C. elegans* (**Figure 4**). First, nematodes were incubated with SNPs, IVN-SNPs, and free IVN for 90 minutes in solution. Second to mimic an in-field applications, IVN-SNPs vs. free IVN were passed through soil columns and the

eluted fractions used for *C. elegans* treatment. For all samples, we performed a modified gel burrowing assay (**Figure 4a**) by transferring the nematodes and casting them in Pluronic F127 in a well-plate[33]. The surface was coated with *E. coli* OP-50 lysate as a food source and to attract the nematodes, and the number of *C. elegans* which penetrated to the surface were counted. Nematode mobility was quantified based on their total track coverage using edge detection (**Figure 4b-d,** and **Figure S9, S10**). The mobility was then estimated using the following equation:

$$v = \frac{1}{N}\frac{A}{A_0}\frac{D}{\Delta t}$$

where v is the approximated mobility, N is the total number of nematodes, A is the area of track coverage, A_0 is the total area in the image, D is the diameter of the well plate, and Δt is the time interval. Data demonstrate efficacy, as measured by reduction in burrowing capabilities of *C. elegans* (**Figure 4e**). Interestingly, the simple approximation of marked surface area as a proxy for number of nematodes on the surface correlated well, suggesting this method could be useful for future high throughput screens at a lower magnification. SNPs alone had no effect which is as expected. When used in solution both IVN-SNPs and free IVN demonstrated efficacy. The highest tested concentration of IVN (10 μM) led to a 4.5-fold reduction in surface velocity and a 6-fold reduction in the number of nematodes on the surface. The largest SNPs (500-2 μm at 5 and 10 mg mL^{-1}) led to a >2-fold reduction in nematode surface velocity and a > 2-fold reduction in number of nematodes on the surface. The smallest SNPs (100-200 nm at 0.1 mg mL^{-1}) yielded a 2.35-fold reduction in nematode surface velocity and 2.9-fold reduction in the number of nematodes on the surface. The IVN concentration in these experiments was normalized, therefore we hypothesize that either the smaller SNPs interact more efficiently with the nematodes, either based on diffusion or higher nanoparticle-to-nematode ratio, and/or that IVN may be more accessible and adsorbed onto the surface of the SNPs (therefore possibly resulting in burst release).

In solution, efficacy of the 500 nm-2 μm IVN-SNPs was ~35% reduced compared to free IVN. However, in the agricultural setting, nematicides need to reach the root-feeding nematodes, therefore a realistic comparison needs to include the soil environment. We added IVN-SNPs vs. free IVN onto a 10 cm soil column and collected fractions before treating *C. elegans*. Only IVN-SNPs resulted in a significant reduction in the number of nematodes and their surface mobility – the treatment successfully paralyzed the nematodes – whereas soluble IVN showed no efficacy, likely because it was lost in the soil (**Figure 4e**). IVN-SNPs formed at 0.1 and 1.0 mg mL^{-1} TMGMV resulted in a 1.36-fold and 1.72-fold reduction on surface velocity and a 1.74-fold and 1.81-fold reduction in nematode number. IVN-SNPs at 5.0 and 10 mg mL^{-1} recovered from the soil columns resulted in a ~2.2 fold reduction in surface velocity and 2.2-2.3-fold reduction in the number of nematodes. From this data we conclude that SNP entrapment of agrochemical cargo enabled soil mobility resulting in effective treatment of nematodes.

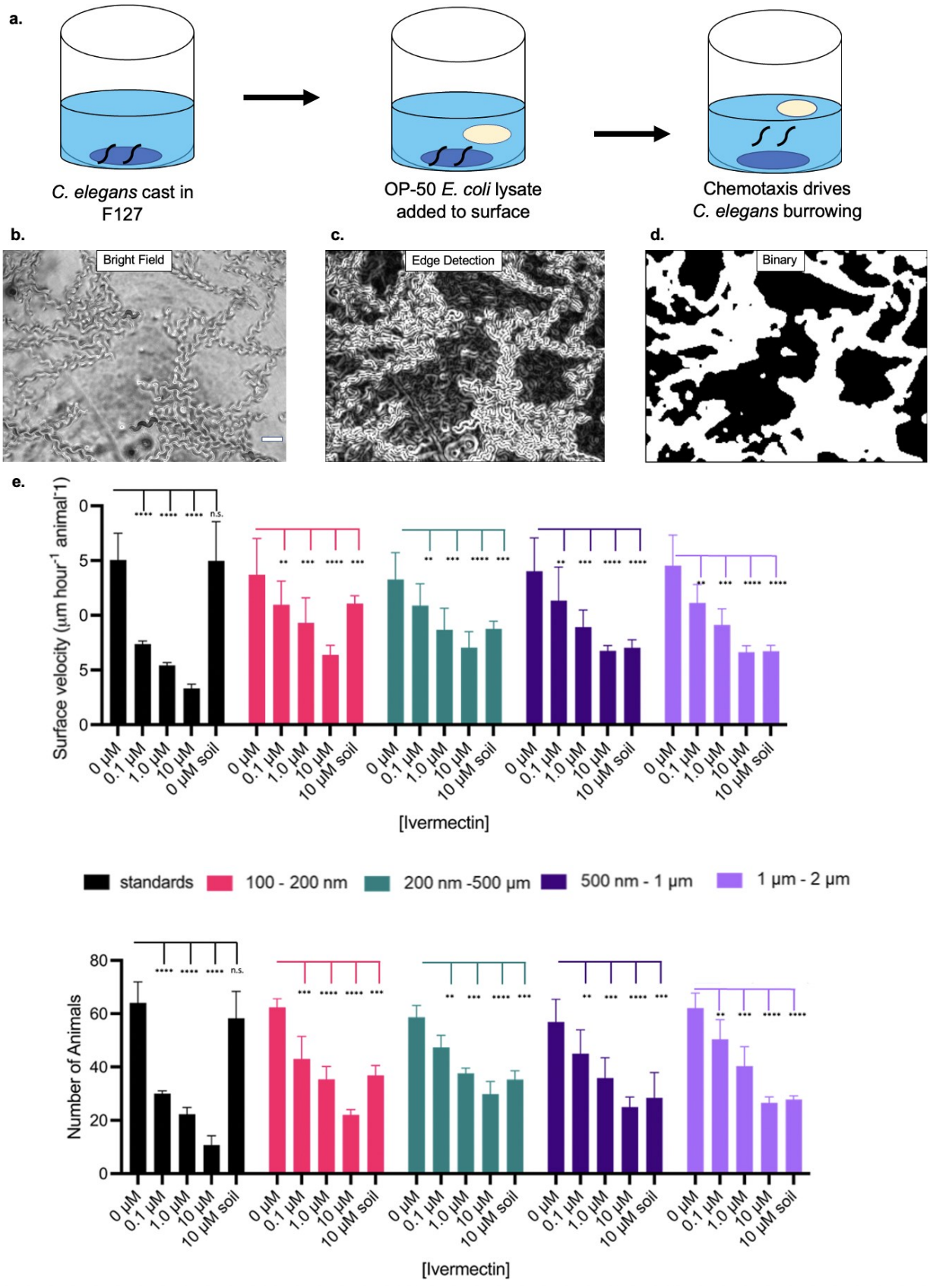
a.
C. elegans cast in F127
OP-50 E. coli lysate added to surface
Chemotaxis drives C. elegans burrowing
b.
Bright Field
c.
Edge Detection
d.
Binary
e.
Surface velocity (µm hour-1 animal-1)
[Ivermectin]
0 µM
0.1 µM
1.0 µM
10 µM
10 µM soil
standards
100 - 200 nm
200 nm -500 µm
500 nm - 1 µm
1 µm - 2 µm
Number of Animals
[Ivermectin]

Figure 4. Assessment of ivermectin SNPs on *C. elegans* paralysis. A schematic of the pluronic F127 gel burrowing assay with an attractant of *E. coli* on the surface (a). Image analysis workflow to identify the area covered by *C. elegans* on the surface of the pluronic F127 gel at 10X magnification; bright field (b), edge detected (c), and binary (d). The calculated surface velocity (e) and number of nematodes (f) for *C. elegans* treated with SNPs at different concentrations of ivermectin in four preparations (N = 3).

In summary, SNP-based encapsulation was highly efficient for soil-based delivery of nematicides. We detailed the phase space for SNP synthesis, showing heating times greater than 30 s and temperatures higher than 90 °C led to SNP formation. SNP sizes were protein concentration dependent, and a size range of SNPs from 100 nm to 2 μm in diameter was synthesized. Mechanistically, it is an interesting question whether a single TMGMV transforms into an SNP, and whether with increasing concentration bundles of TMGMV transform into larger SNPs – or whether TMGMV disassembles into CPs which then aggregate into SNPs. Future simulations and experimental studies should be designed to probe the dynamics of TMGMV disassembled and SNP assembly. We demonstrated effective encapsulation of Cy5 and ivermectin into SNPs during thermal TMGMV-to-SNP transition. Finding a medium, like acetonitrile, which can be heated to > 90 °C and maintain target molecule solubility is important for effective encapsulation. Acetonitrile enhanced solubility of the active ingredient and improved SNP synthesis, likely by aiding destabilization of the TMGMV assembly. Future applications may require more sustainable cosolvents. Importantly, we demonstrate efficient active ingredient loading and co-delivery in soil to target root-feeding nematodes. While free ivermectin was not effective after soil passage, IVN-SNPs facilitated soil mobility and efficacy against *C. elegans*. We envision these techniques could find applications beyond pesticide delivery in soil and be extended for foliar active ingredient delivery. TMGMV itself has already been approved by the EPA as a bioherbicide and this non-covalent encapsulation could to streamline the regulatory process. The use of one-pot synthesis methods is expected to yield in a scalable industry process.

Supporting Information: Additional experimental details, materials, methods, and supporting figures including additional SEM images of SNPs and image analysis, proteomic analysis of SNP proteins, additional soil mobility measurements, standard curve for ivermectin ELISA, CD spectra, images of *C. elegans* on Pluronic gel surface.

Acknowledgments:

This work was sponsored in part by the UC San Diego Materials Research Science and Engineering Center (UCSD MRSEC), supported by the National Science Foundation (Grant DMR-2011924, to NFS and JKP). This work is supported in part by grants from USDA, NIFA-2020-67021-31255 (to NFS) and NIFA-2022-67012-36698 (to AAC). This work was also supported by the National Science Foundation CMMI 1901713 (to JKP). The authors would like to acknowledge Majid Ghassemian of the Biomolecular and Proteomics Mass Spectrometry Facility (BPMSF) at the University of California San Diego for his assistance and use of facilities. The BPMSF is funded by the NIH under grants S10 OD016234 (Synapt-HDX-MS) and S10 OD021724 (LUMOS Orbi-Trap). This work was performed in part at the San Diego Nanotechnology Infrastructure (SDNI) of University of California San Diego, a member of the National Nanotechnology Coordinated Infrastructure (NNCI), which is supported by the National Science Foundation (Grant ECCS-1542148). This work was performed in part at the University of California San Diego Department of Neurosciences Microscopy Core, supported by the National Institutes of Health (NINDS P30NS047101). The authors thank Udhaya Pooranam Venkateswaran, Justin McCaskill, Sabrina Chang Liao, and George Goldenfeld for their support in this project. The authors thank Dr. Emily Troemel and Mario Sarmiento (UCSD) for providing the nematodes for this study.

References:

1. Agriculture, U. N. F. a. *Hunger and food insecurity*; United Nations: https://www.fao.org/hunger/en/, 2023. Accessed June 12th 2023.
2. Damalas, C. A.; Eleftherohorinos, I. G., Pesticide Exposure, Safety Issues, and Risk Assessment Indicators. *Int. J. Environ. Res. Public Health* **2011,** *8* (5), 1402-19.
3. Rae, C. S.; Khor, I. W.; Wang, Q.; Destito, G.; Gonzalez, M. J.; Singh, P.; Thomas, D. M.; Estrada, M. N.; Powell, E.; Finn, M. G.; Manchester, M., Systemic trafficking of plant virus nanoparticles in mice via the oral route. *Virology* **2005,** *343* (2), 224-35.
4. Yan, J.; Huang, K.; Wang, Y.; Liu, S., Study on Anti-Pollution Nano-Preparation of Dimethomorph and its Performance. *Chin. Sci. Bull.* **2005,** *50* (2), 108-112.
5. Nuruzzaman, M.; Rahman, M. M.; Liu, Y.; Naidu, R., Nanoencapsulation, Nano-guard for Pesticides: A New Window for Safe Application. *J. Agric. Food. Chem.* **2016,** *64* (7), 1447-83.
6. Gupta, R.; Xie, H., Nanoparticles in Daily Life: Applications, Toxicity and Regulations. *J Environ Pathol Toxicol Oncol* **2018,** *37* (3), 209-230.
7. Brown, D. J.; MacFarlane, S. A., 'Worms' that transmit viruses. *Biologist (London)* **2001,** *48* (1), 35-40.
8. Gray, S. M., Plant virus proteins involved in natural vector transmission. *Trends Microbiol* **1996,** *4* (7), 259-64.
9. Cao, J.; Guenther, R. H.; Sit, T. L.; Lommel, S. A.; Opperman, C. H.; Willoughby, J. A., Development of abamectin loaded plant virus nanoparticles for efficacious plant parasitic nematode control. *ACS Appl Mater Interfaces* **2015,** *7* (18), 9546-53.
10. Gonzalez-Gamboa, I.; Caparco, A. A.; McCaskill, J. M.; Steinmetz, N. F., Bioconjugation Strategies for Tobacco Mild Green Mosaic Virus. *Chembiochem* **2022,** *23* (18), e202200323.
11. Chariou, P. L.; Dogan, A. B.; Welsh, A. G.; Saidel, G. M.; Baskaran, H.; Steinmetz, N. F., Soil mobility of synthetic and virus-based model nanopesticides. *Nat Nanotechnol* **2019,** *14* (7), 712-718.
12. Ferrell, J.; Charudattan, R.; Elliott, M.; Hiebert, E., Effects of Selected Herbicides on the Efficacy of Tobacco Mild Green Mosaic Virus to Control Tropical Soda Apple (Solanum Viarum). *Weed Sci.* **2008,** *56* (1), 128-132.
13. Charudattan, R.; Pettersen, M. S.; Hiebert, E. Use of Tobacco Mild Grenn Mosaic Virus (TMGMV) Mediated Lethal Hypersensitive Response (HR) as a Novel Method of Weed Control. **2009**. Patent US20040162220A1
14. Charudattan, R.; Hiebert, E., A Plant Virus as a Bioherbicide for Tropical Soda Apple, Solanum Viarum. *Outlooks on Pest Management* **2007,** *18* (4), 167-171.
15. Lomonossoff, G. P.; Wege, C., TMV Particles: The Journey From Fundamental Studies to Bionanotechnology Applications. *Adv Virus Res* **2018,** *102*, 149-176.
16. Shin, M. D.; Hochberg, J. D.; Pokorski, J. K.; Steinmetz, N. F., Bioconjugation of Active Ingredients to Plant Viral Nanoparticles Is Enhanced by Preincubation with a Pluronic F127 Polymer Scaffold. *ACS Applied Materials & Interfaces* **2021,** *13* (50), 59618-59632.
17. Nikitin, N.; Ksenofontov, A.; Trifonova, E.; Arkhipenko, M.; Petrova, E.; Kondakova, O.; Kirpichnikov, M.; Atabekov, J.; Dobrov, E.; Karpova, O., Thermal conversion of filamentous potato virus X into spherical particles with different properties from virions. *FEBS Letters* **2016,** *590* (10), 1543-1551.
18. Manukhova, T. I.; Evtushenko, E. A.; Ksenofontov, A. L.; Arutyunyan, A. M.; Kovalenko, A. O.; Nikitin, N. A.; Karpova, O. V., Thermal remodelling of Alternanthera mosaic virus virions and virus-like particles into protein spherical particles. *PLOS ONE* **2021,** *16* (7), e0255378.

19. Atabekov, J.; Nikitin, N.; Arkhipenko, M.; Chirkov, S.; Karpova, O., Thermal transition of native tobacco mosaic virus and RNA-free viral proteins into spherical nanoparticles. *J Gen Virol* **2011,** *92* (Pt 2), 453-6.
20. Bruckman, M. A.; Czapar, A. E.; VanMeter, A.; Randolph, L. N.; Steinmetz, N. F., Tobacco mosaic virus-based protein nanoparticles and nanorods for chemotherapy delivery targeting breast cancer. *Journal of Controlled Release* **2016,** *231*, 103-113.
21. Bruckman, M. A.; Hern, S.; Jiang, K.; Flask, C. A.; Yu, X.; Steinmetz, N. F., Tobacco mosaic virus rods and spheres as supramolecular high-relaxivity MRI contrast agents. *Journal of Materials Chemistry B* **2013,** *1* (10), 1482-1490.
22. Bruckman, M. A.; VanMeter, A.; Steinmetz, N. F., Nanomanufacturing of Tobacco Mosaic Virus-Based Spherical Biomaterials Using a Continuous Flow Method. *ACS Biomaterials Science & Engineering* **2015,** *1* (1), 13-18.
23. Deutsch, D. G., Effect of prolonged 100°C heat treatment in sodium dodecyl sulfate upon peptide bond cleavage. *Analytical Biochemistry* **1976,** *71* (1), 300-303.
24. Kowit, J. D.; Maloney, J., Protein cleavage by boiling in sodium dodecyl sulfate prior to electrophoresis. *Analytical Biochemistry* **1982,** *123* (1), 86-93.
25. Kurien, B. T.; Scofield, R. H., Common Artifacts and Mistakes Made in Electrophoresis. In *Protein Electrophoresis: Methods and Protocols*, Kurien, B. T.; Scofield, R. H., Eds. Humana Press: Totowa, NJ, 2012; pp 633-640.
26. Arias-Estévez, M.; López-Periago, E.; Martínez-Carballo, E.; Simal-Gándara, J.; Mejuto, J.-C.; García-Río, L., The mobility and degradation of pesticides in soils and the pollution of groundwater resources. *Agriculture, Ecosystems & Environment* **2008,** *123* (4), 247-260.
27. Brewer, A.; Dror, I.; Berkowitz, B., The Mobility of Plastic Nanoparticles in Aqueous and Soil Environments: A Critical Review. *ACS ES&T Water* **2021,** *1* (1), 48-57.
28. Chariou, P. L.; Dogan, A. B.; Welsh, A. G.; Saidel, G. M.; Baskaran, H.; Steinmetz, N. F., Soil mobility of synthetic and virus-based model nanopesticides. *Nature Nanotechnology* **2019,** *14* (7), 712-718.
29. Katagi, T., Soil Column Leaching of Pesticides. In *Reviews of Environmental Contamination and Toxicology Volume 221*, Whitacre, D. M., Ed. Springer New York: New York, NY, 2013; pp 1-105.
30. Dobrov, E. N.; Nikitin, N. A.; Trifonova, E. A.; Parshina, E. Y.; Makarov, V. V.; Maksimov, G. V.; Karpova, O. V.; Atabekov, J. G., β-structure of the coat protein subunits in spherical particles generated by tobacco mosaic virus thermal denaturation. *Journal of Biomolecular Structure and Dynamics* **2014,** *32* (5), 701-708.
31. Della Pelle, G.; Delgado López, A.; Salord Fiol, M.; Kostevšek, N., Cyanine Dyes for Photo-Thermal Therapy: A Comparison of Synthetic Liposomes and Natural Erythrocyte-Based Carriers. *International Journal of Molecular Sciences* **2021,** *22* (13), 6914.
32. Chariou, P. L.; Steinmetz, N. F., Delivery of Pesticides to Plant Parasitic Nematodes Using Tobacco Mild Green Mosaic Virus as a Nanocarrier. *ACS Nano* **2017,** *11* (5), 4719-4730.
33. Lesanpezeshki, L.; Hewitt, J. E.; Laranjeiro, R.; Antebi, A.; Driscoll, M.; Szewczyk, N. J.; Blawzdziewicz, J.; Lacerda, C. M. R.; Vanapalli, S. A., Pluronic gel-based burrowing assay for rapid assessment of neuromuscular health in C. elegans. *Scientific Reports* **2019,** *9* (1), 15246.

TOC Graphic: